DOI: 10.61782/fa.2023.0036

forum acusticum 2023

AIR JET DYNAMICS IN A FLUE INSTRUMENT

N. Giordano[1*] **and K. L. Saenger**[1,2]
[1] Department of Physics, Auburn University, USA
[2] Independent Laboratory, Ossining, New York, USA

ABSTRACT

In a flue instrument such as the recorder, an air jet undergoes an oscillatory motion with the jet directed alternately to either side of the labium. The dynamics of that oscillation, including the trajectory followed by the jet, depends on the jet speed, a parameter controlled by the blowing pressure. We describe new studies of how the jet oscillations depend on blowing pressure in a recorder. Small Pitot-tube-like pressure sensors are installed in close proximity to the labium tip of a soprano recorder, with two sensors above the tip and two below. The pressures at these four locations give the time-averaged spatial profile of the air jet. This profile is observed to change as the blowing pressure is increased from low values, where the note C5 is produced, to high pressures where the note an octave higher, C6, is sounded. Additionally, it was found that different spatial profiles are found for C5 and C6 even when they are produced at the same blowing pressure. We have compared the experimentally measured jet profiles with the results of Navier-Stokes-based simulations of the same instrument geometry under the same blowing conditions, and find similar variations in the time-averaged jet profiles. The simulations also give the time-resolved jet profiles, which provide further insight into this behavior.

Keywords: *recorder, air jet dynamics, flue instruments, regime change, pitot sensors*

[*] ***Corresponding author***: *njg0003@auburn.edu.*

1. INTRODUCTION

Flue instruments such as the recorder have been the subject of many different experimental, theoretical, and modeling studies, and much is known about the way they produce musical tones. (There is a vast literature in this area. Some references that are particularly relevant to our work can be found in [1,2,3,4,5] and references contained therein.) However, there are still interesting and unanswered questions concerning the behavior of these instruments. In recent work [6,7] we have investigated the phenomenon of regime change in the recorder. Regime change occurs when the blowing pressure is increased after starting from a low value, so as to cause the instrument to "jump" to a higher note, typically an octave higher. Regime change can also occur when the blowing pressure is decreased and the note jumps down an octave. In [6] we showed that the regime change transition can exhibit hysteresis; that is, the transition pressure can depend on the blowing history. In [7] it was shown that the time-averaged profile of the air jet appears to change abruptly at the transition. Furthermore, by briefly interrupting or deflecting the air jet (e.g., by placing an obstruction near the labium) it is possible to cause regime change when the blowing conditions are in the hysteresis region. One goal of the present work is to characterize the jet trajectories associated with each regime; another is to better understand how changes in these trajectories might be connected with regime change. To this end we have employed small Pitot-tube-like pressure sensors (referred to below as Pitot sensors) placed near the labium to measure the time-averaged spatial variation of the pressure under different blowing conditions. To complement the experiments we have used Navier-Stokes-based simulations to calculate the Pitot pressure under similar blowing conditions, and to also visualize theoretically the time dependence of the air jet trajectory in different oscillation regimes. Our ultimate objective is to understand the dynamics of the jet trajectory during the

transitions between different notes, in this case between C5 and C6.

2. EXPERIMENTAL METHOD

An artificial blowing machine [6,7,8] was used to play a Yamaha model YRS-20 soprano recorder, a common student instrument. This instrument is a transparent version of the YRS-23 which we have studied in other work [6,7,8]. The blowing pressure, i.e., the pressure just upstream from the input to the channel of the recorder (Fig. 1), was held fixed while the flow speed through the channel (inferred from the measured flow rate and the 1 mm x 10 mm cross sectional area of the channel exit aperture) and the sound pressure outside the instrument were measured and recorded. Small Pitot sensors were positioned near the tip of the labium, with two sensors above and two below as shown in Fig. 1. The sensors were steel tubes with inner and outer diameters of 1.2 mm and 1.7 mm respectively. The open ends of tubes 1 and 2 were facing the -*x* direction, while the open ends of tubes 3 and 4 were perpendicular to the sloped edge of the labium. The transparent walls of the YRS-20 made accurate and reproducible placement of sensors 1 and 2 easier than with the YRS-23 instrument. Relevant dimensions of the instrument (Fig. 1) include the height of the channel along *y* (1.0 mm), the width of the channel along *z* (10 mm), and the distance from the exit of the channel to the labium (4.0 mm). The labium tip in the YRS-20 instrument is aligned with the bottom of the channel. The channel has a chamfer on its bottom edge of about 0.5 mm in length. The tone holes were closed for all of the measurements described in this paper, so the note produced at low blowing pressures was C5 (fundamental frequency approximately 523 Hz), one octave above middle C.

Each Pitot tube was connected to a pressure gauge so that the pressures at all four sensors could be measured simultaneously. The response times of the pressure gauges were such that we could only measure the time averaged pressure. All of the measurements reported in this paper were with the Pitot sensors positioned approximately 1 mm downstream from the tip of the labium, as shown in Fig. 1. With these positions, the sound of the instrument was essentially the same as for an instrument without sensors. We also verified that the readings of sensors 1, 2, and 3 were not affected by the presence or absence of sensor 4 (the only sensor that could be removed without disturbing the positions of the others). In separate measurements it was found that positioning the Pitot sensors in the window region (i.e., upstream from the labium) did have a noticeable effect on the sound.

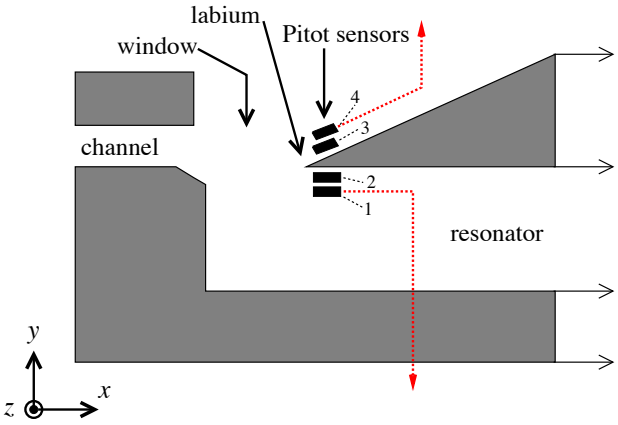

Figure 1. Schematic of the YRS-20 recorder with the Pitot tube sensors. Not to scale; important dimensions are given in the text. The resonator extends far to the right, beyond the edge of the figure. The red dotted lines show thin steel portions of the tubing that connects sensors 1 and 4 to pressure gauges; the other two sensors are connected in a similar manner. For sensors 1 and 2 these tubes pass through sealed fittings in the bottom of the resonator.

3. SIMULATION METHOD

The simulations involved an explicit finite difference time domain solution of the compressible Navier-Stokes equations in three dimensions. This was accomplished using custom computer code written for parallel high-performance computers, as described elsewhere [9]. The MacCormack method [10] was used along with the addition of artificial viscosity [11] to suppress turbulent instabilities, as described in [9]. A nonuniform Cartesian grid was used with a grid spacing of 0.1 mm in the vicinity of the channel, window, and labium. The model used in the simulation was patterned after that of the YRS-20 instrument, with similar dimensions for the channel height and width, window length, labium angle, and resonator length. The model had a resonator tube similar in length to that of the YRS-20, with an inner diameter that tapered in a similar manner from approximately 12 mm near the labium to 8.5 mm at the

open end. The model contained tone holes but all were closed for the results reported here. The blowing was established by imposing a specified value of the air speed in the *x* direction in the first several mm of the channel (to the left in Fig. 1). The simulations yielded the full flow field, the values of the density and the three components of the air velocity, as a function of space and time.

To compare with the Pitot pressures of the experimental sensors, the simulation results for the pressures *p* at the Pitot tubes were calculated by computing

$$p = \langle \rho(air) \times v(perp)^2 \rangle \quad (1)$$

where $\rho(air)$ is the density of air at room pressure, $v(perp)$ is the component of the air velocity perpendicular to the face of the sensor, and the angle brackets indicate an average over typically 20 complete oscillation cycles after reaching steady state. The sign in (1), which can be derived from the Navier-Stokes equations, assumes flow into the sensor, which was found to always be the case in our simulations. Since the simulations yielded the flow field on time scales much faster than an oscillation cycle for C5 or C6, it was also possible to produce movies of the effectively instantaneous flow field. Images from such movies will be shown below. Lastly, we note that the simulations did not include the solid portions of the sensors or their connecting tubing.

4. RESULTS

4.1 Pitot Pressure Profiles

Figure 2 shows experimental results for the Pitot pressure profiles measured with different values of the average speed of the air jet (here and below we give the average speed, recognizing that this speed varies across the height of the channel due to Poiseuille's law). Recall that sensors 2 and 3 are just below and above the labium, so these results show that the time averaged Pitot pressure is largest nearest the tip of the labium. The filled symbols connected with solid lines show data when the note sounded is C5, while the open symbols and dashed lines show measurements in the C6 regime. Here the regime change transition occurs at a jet speed near 10 m/s, and hysteresis (as described in [6] and [7]) is found at jet speeds in that neighborhood. As examples, either C5 or C6 can be produced with jet speeds of 9.1 and 10.6 m/s, depending on the blowing history.

From Fig. 2 we see that the Pitot pressures generally increase as the jet speed is increased, particularly at sensors 2 and 3. While there are only four sensors, we can still discern noticeable changes in the shape of the pressure profile. Below the regime change transition the profile is peaked at sensor 3, that is, just above the tip of the labium, whereas just above the transition the profile is almost symmetric, with the pressures at sensors 2 and 3 more nearly equal. The behaviors at 9.1 and 10.6 m/s are especially interesting. At these jet speeds either C5 or C6 can be obtained (through different blowing histories), with distinctly different results, and these differences were reproducible over multiple cycles of C5-C6 switching. This all suggests that regime change from C5 to C6 is accompanied by an abrupt change in the time-averaged profile of the air jet.

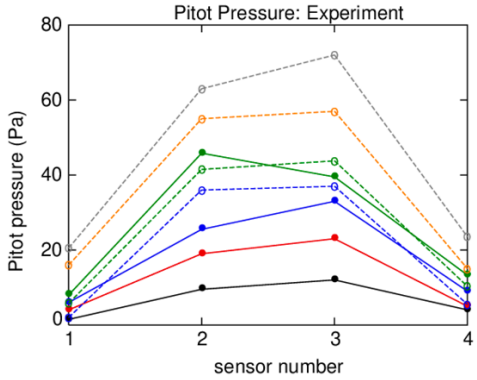

Figure 2. Experimental Pitot sensor results. Solid symbols and solid lines show data in the C5 regime; dashed lines and open symbols show data in the C6 regime. The average jet speeds in m/s were black: 5.1 (C5); red: 8.0 (C5); blue: 9.1 (C5 and C6); green: 10.6 (C5 and C6); orange: 13.3 (C6); and grey: 15.1 (C6).

Figure 3 shows simulation results for the Pitot pressure profiles under blowing conditions similar to those used in the experiment. In Fig. 3 the solid symbols and solid lines show data in the C5 regime, while the open symbols and dashed lines are for data in the C6 regime. Hysteresis is found with jet speeds near 11 m/s; i.e., at this and nearby jet speeds either C5 or C6 tones could be produced, depending on the blowing history. The simulation exhibits most of the main features seen experimentally: (1) The experiment and simulation show hysteresis at similar jet speeds (10 m/s and 11 m/s respectively); (2) The absolute Pitot pressures for the center two probes agree to better than 30%; and (3) The transition from C5 to C6 occurs at a Pitot pressure for

sensors 2 and 3 of about 35 Pa, which is very close to the value found in the experiments.

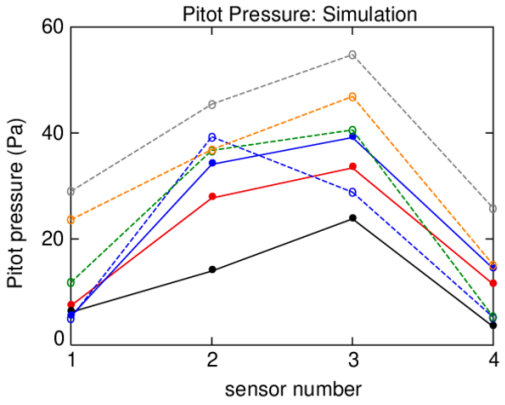

Figure 3. Simulated Pitot sensor results. Solid symbols and solid lines show data in the C5 regime; dashed lines and open symbols show data in the C6 regime. The average jet speeds in m/s were black: 8.5 (C5); red: 10.6 (C5); blue: 11.3 (C5 and C6); green: 12.0 (C6); orange: 14.2 (C6); and grey: 16.3 (C6).

4.2 Jet dynamics in the hysteresis region

Both the experiments and the simulations exhibit a hysteresis region; that is, a range of blowing speeds at which the instrument can produce either C5 or C6, depending on the blowing history. In [7] it was shown that a transition between these two notes can be produced by interrupting the flow in particular ways for periods of order 0.5 to 1 s. There are different ways this can be done reproducibly. Here we consider two such ways. (1) Inserting a thin (of order 1 mm thick) sheet of plastic in the window region, oriented parallel to the *y*-*z* plane in Fig. 1, so as to briefly obstruct the flow in the window region over approximately the central half of the channel [12]. This was found to cause a transition from C6 to C5. (2) Briefly inserting a wider sheet of plastic (again oriented parallel to the *y*-*z* plane) to temporarily block the channel over its full length. This was found to cause a transition from C5 to C6. To account for these different behaviors we now go beyond the time-averaged results in Fig. 2 and 3, and use the simulations to explore the spatiotemporal variations of the air jet. We start with the C6 to C5 transition.

The simulations give the density and flow velocity as functions of position and time. From those data we have calculated streamlines of the flow and produced movies showing the time dependence of the streamline patterns. Images showing the density and/or flow as derived from experiments (e.g., in [2,3,5,13]) or from simulations (e.g., [9,14,15,16,17,18]) have been presented by previous workers. However, essentially all of those images have been limited to two dimensions, in the *x*-*y* plane of Fig.1. Notable exceptions are the simulations in [14] and [16] but these show much less detail than the streamline images that we next describe. As we will see, there is interesting 3D structure in the flow that has not been previously recognized.

Figures 4 and 5 show streamlines derived from two of our simulations for a jet speed in the hysteresis region. Figure 4 shows images from a movie with the instrument sounding C5, while Fig. 5 shows corresponding images from a movie at the *same* air jet speed with the instrument sounding C6. We first consider the results in the C5 region, Fig. 4.

The image in Figs. 4a shows a side view of the streamlines calculated by integrating the flow velocity starting in the channel where the jet velocity is parallel to the *x* direction, that is, directed from left to right (in Fig. 1). The color of each streamline varies according to the component of the velocity along the *y* direction (see again Fig. 1), the component in the vertical direction *at this moment on that streamline*. This image is part of a movie that shows how the pattern of streamlines vary with time during the course of an oscillation cycle. The particular image in Fig. 4a was recorded at an instant when the jet trajectory was, on average, at its lowest relative to the labium, and shows the streamlines as they "travel" out of the channel, through the window region, past the labium, and downstream either into the resonator or above the labium. Most of these streamlines travel downward as they pass beneath the labium and are thus colored blue. A few streamlines below and just beyond the outlet of the channel are red, as a vortex has developed in that region of the window. A small number of streamlines pass above the labium, and these alternate in color between red and blue as v_y on these lines oscillates in sign.

In order to understand the geometry of the streamlines as they travel from the channel and through the window region before they reach the labium, Fig. 4b shows a view looking back from the center of the resonator toward the upstream end of the instrument. That is, the plane of this image is parallel to the *y*-*z* plane in Fig. 1. Here we show streamlines at the same instant as in Fig. 4a, but we have terminated the streamlines when they reach the labium tip (see part (a) of the figure). The pattern in Fig. 4b shows

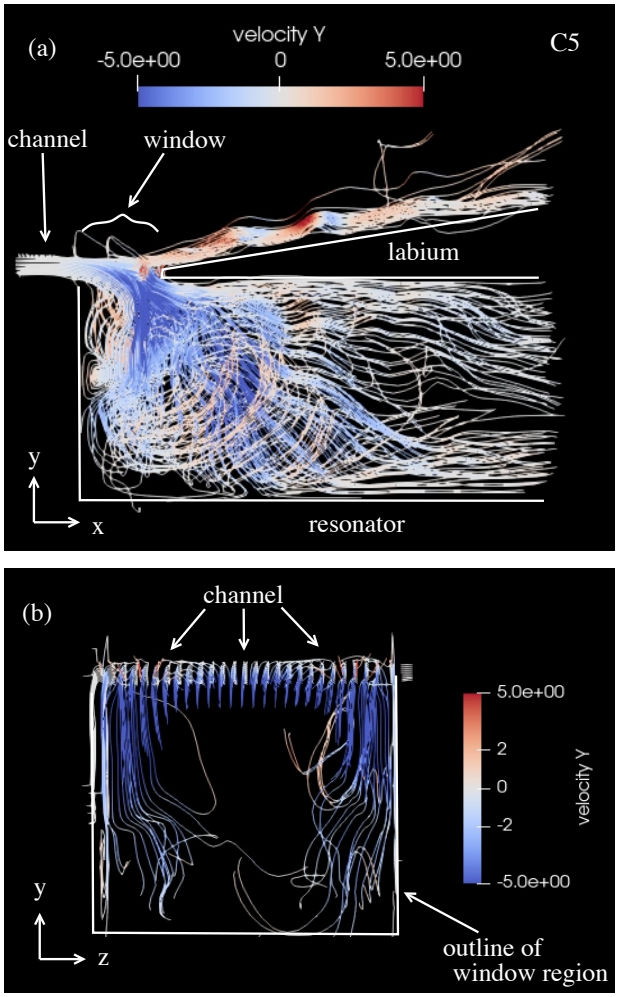

Figure 4. Flow streamlines at one instant in an oscillation cycle with the instrument sounding C5 and an average jet speed of 11.8 m/s. Streamline color is determined by the component of the velocity along the vertical (the *y* direction in Fig. 1). (a) Side view showing the flow as it moves from the channel through the window region, past the labium tip and then into the resonator or above the labium. (b) View at the same instant as part (a) but now looking from the center of resonator back toward the channel. Here only the streamlines in the channel and window region are shown, in order to show just the flow as it leaves the channel and passes through the window. In this region the cross section of the recorder is rectangular.

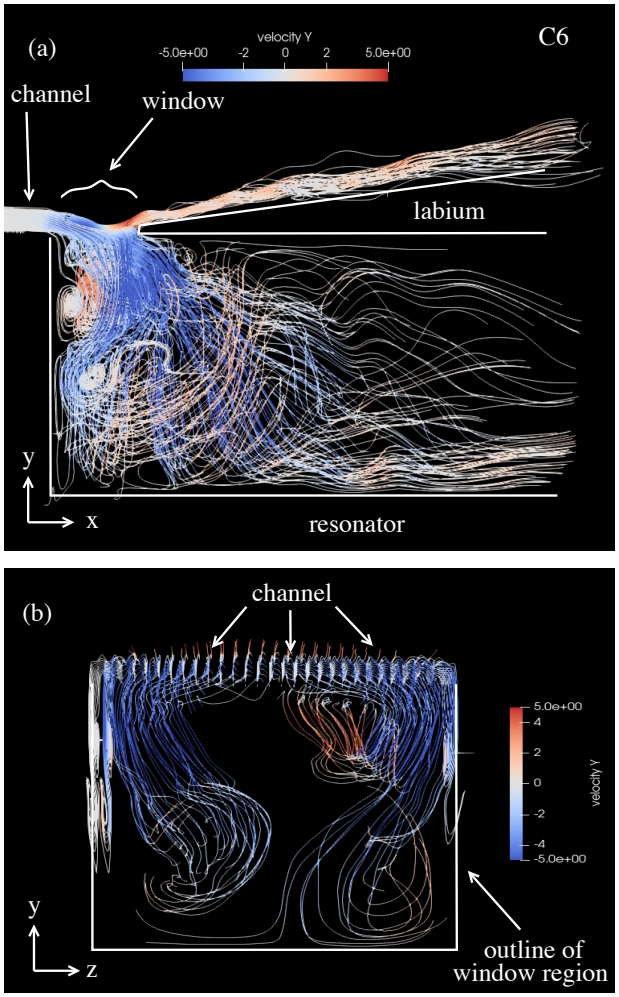

Figure 5. Flow streamlines at one instant in an oscillation cycle with the instrument sounding C6 and an average jet speed of 11.8 m/s. (a) Side view showing the flow as it moves from the channel through the window region, past the labium tip and then into the resonator or above the labium. (b) View at the same instant as part (a) but now looking from the center of resonator back toward the channel. See the caption for Fig. 4 and the text for more explanation of these images.

what was, for us, an unexpected result. At this moment the flow travels predominantly along the edges of the window, with much less flux in the center of the window. Other images of the streamlines (not included here) show that as it progresses downstream, beneath the labium, the flow is directed from the edges toward the center of the resonator.

On the far right in Fig. 4a the streamlines and flow more nearly fill the resonator.

An important result from the streamline movies in the C5 regime is that the flow through the window region is predominantly along the edges of the instrument. This is *not* found when the tone is in the C6 region. Comparison images from the C6 streamline movie are shown in Fig. 5; part (a) of figure shows a side view when the jet trajectory was, on average, at its lowest relative to the labium while Fig. 5b shows an image at the same instant looking upstream from the resonator and with the streamlines terminated when they reach the labium. While the flow in Fig. 5b is again largest at the edges of the instrument, the flow now extends further into the center of the window than in the C5 case (Fig. 4b). Examination of the full movies shows that during each complete oscillation cycle there is, on average, much more flow in the center of the window region for the C6 tone than with the C5 tone.

We suggest that these two flow patterns can explain why the flow interruption (#1) described above could induce a transition from C6 to C5. That interruption employed an obstacle in the center of the window region, which would presumably have relatively little effect on the flow pattern in Fig. 4b, but block a larger fraction of the flow in Fig. 5b. It then seems plausible that the result would be to leave the system in a flow state that gives a C5 tone. This is a qualitative argument, based only on the general appearance of the flow patterns. A more quantitative argument will have to address what happens while the flow is interrupted and the detailed trajectory that the flow pattern takes in a multidimensional pattern space. These are problems we hope to address in the future.

We next consider the interruption (#2) described above that produces a C5 to C6 transition. In that case, the flow from the channel was largely and briefly blocked. Experimentally this blockage caused a short period of silence followed by a momentary spike in the blowing pressure, due to a build-up in pressure in the region just upstream from the input to the channel. While a temporary overshoot in the blowing pressure (and hence in the jet speed) could be responsible for the resulting C6 state, the simulations suggest that the critical factor is the *rate* at which the blowing speed increases to its final value. In our simulation, we assumed that the jet speed was reduced to zero and then allowed to increase rapidly back to the previous speed. We modeled this by starting with a jet speed of zero and then rapidly increasing it to a final value [19]. In Fig. 6a we show the behavior of the sound pressure outside the instrument (as would be heard by a listener) when the jet speed was increased gradually, in small steps from well below the hysteresis region, as might be done by a player. In this case the note C5 is produced. Figure 6b shows the result when the jet speed is increased quickly (a 5 ms ramp-up time) from zero to the same final value. In this case the note C6 is produced, a clear indication of the importance of the ramp rate. However, further simulations are

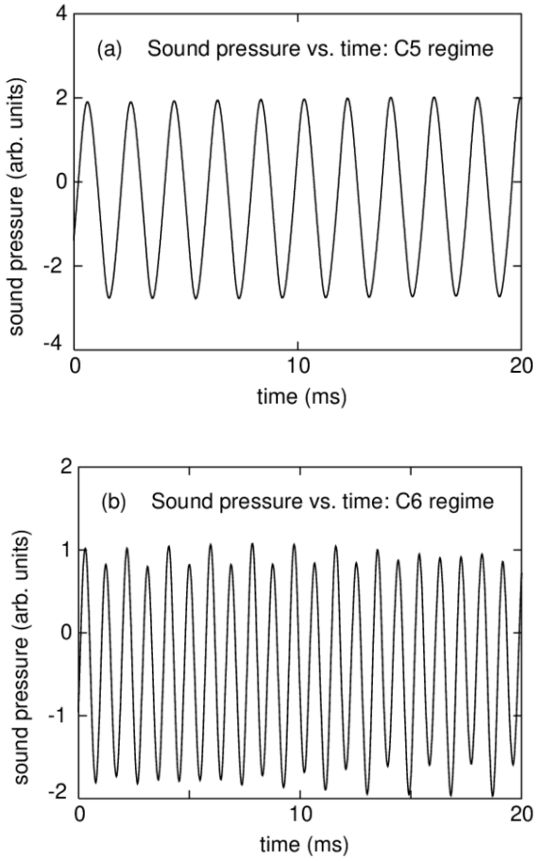

Figure 6. Sound pressure as a function of time in the hysteresis region. In both cases the jet speed was 11.8 m/s. The only difference was in the previous history of the jet speed. In (a) the jet speed was increased gradually from a value below the hysteresis region and then held fixed, resulting in a C5 tone (period ~1.9 ms). In (b) the speed was increased abruptly from zero to its final value resulting in a C6 tone (period ~ 0.96 ms). In (b) there is a small but noticeable spectral component at approximately 520 Hz. These pressure-time waveforms were calculated in the simulations used to produce the movies discussed in connection with Figs. 4 and 5.

needed to explore quantitatively how the streamlines evolve with different ramping rates.

5. CONCLUSIONS

We have studied regime change in a soprano recorder using a combination of experiments and simulations. The experiments have used small Pitot tube sensors to measure the time-averaged profile of the air jet near the labium. The profile is observed to change as the jet velocity is increased through the regime change transition from C5 to C6. Most importantly, in the hysteretic region we find that the pressure profiles in these two regimes are quite different even at the *same* jet speeds. Results for the jet profile are obtained using Navier-Stokes-based simulations, and good agreement is found with the experiments. The simulations are also used to understand, in a qualitative sense, how interruptions of the flow can induce regime change. While the simulations are consistent with the experiments, the explanations in Sec. 4.2 should be viewed as plausibility arguments. More work is needed to understand quantitatively the jet dynamics involved in the regime change transition, either through time-resolved imaging, or simulations that explicitly include the way the air jet is interrupted, or both. Our visualizations of the flow using streamlines have also revealed previously overlooked aspects of the three-dimensional flow patterns near the labium in a flue instrument that deserve further study.

6. ACKNOWLEDGMENTS

Work supported in part by U.S. National Science Foundation grant PHY1806231.

7. REFERENCES

[1] B. Fabre and A. Hirschberg, "Physical modeling of flue instruments: A review of lumped models," *Acustica-Acta Acustica* **86**, 599-610 (2000).

[2] C. Ségoufin, B. Fabre, M. P. Verge, A. Hirschberg, and A. P. J. Wijnands, "Experimental study of the influence of the mouth geometry on sound production in a recorder-like instrument: Windway length and chamfers," *Acustica-Acta Acustica* **86**, 649-661 (2000).

[3] P. de la Cuadra, "The sound of oscillating air jets: Physics, modeling and simulation in flute-like instruments," Ph.D. Thesis, Stanford University, (2006).

[4] R. Aubray, B. Fabre, and P-Y. Lagrée, *J. Acoust. Soc. Amer.* **131**, 1574-1585 (2012); doi.org/10.1121/1.3672815.

[5] B. Fabre, J. Gilbert, A. Hirschberg, and X. Pelorson, "Aeroacoustics of Musical Instruments," *Annu. Rev. Fluid. Mech.* **44**, 1-25 (2012); 10.1146/annurev-fluid-120710-101031.

[6] N. Giordano, K. L. Saenger, and J. W. Thacker, "Study of hysteretic behavior in the recorder," *Proc. Mtgs. Acoust.* **49**, 035002 (2022); doi: 10.1121/2.0001644.

[7] K. L. Saenger, "Regime-change-induced modification of jet flow in flute-like instruments with a hysteresis region," *Proc. Mtgs. Acoust.* **49**, 035003 (2022); doi: 10.1121/2.0001657.

[8] N. Giordano and K. L. Saenger, "Study of `half-integer' harmonics in recorder tones and some speculations about their orgin," *J. Acoust. Soc. Amer.* **154**, 2917-2927 (2023); doi.org/10.1121/10.0022327.

[9] N. Giordano, "Simulation studies of a recorder in three dimensions," *J. Acoust. Soc. Amer.* **135**, 906-916 (2014); doi.org/10.1121/1.4861249.

[10] R. W. MacCormack, "The effect of viscosity in hypervelocity impact cratering," *AAIA* Paper **69–354**, 1–7 (1969).

[11] A. Jameson, W. Schmidt, and E. Turkel, "Numerical solution of the Euler equations by finite volume methods using Runge Kutta time stepping schemes," *AAIA* Paper **81–1289**, 1–14 (1981).

[12] To give a bit more detail, we observed this behavior by inserting a narrow strip of plastic having a thickness of 0.8 to 2 mm and a width of ~6 to 9 mm into the downstream half of the window region along a vertical plane (i.e., parallel to the *y-z* plane in Fig. 1) until the bottom edge of the strip was approximately even with the labium tip. This briefly deflected the top half of the flow away from the central portion of the labium tip and caused a transition from C6 to C5.

[13] S. Yoshikawa, "A pictorial analysis of jet and vortex behaviours during attack transients in organ pipe models," *Acustica-Acta Acustica* **86**, 623-633 (2000).

[14] H. Kühnelt, "Vortex sound in recorder- and flute-like instruments: Numerical simulation and analysis," Proceedings of the International Symposium on Musical Acoustics (ISMA 2007), (2007).

[15] M. Miyamoto, Y. Ito, T. Iwasaki, T. Akamura, K. Takahashi, T. Takami, T. Kobayashi, A. Nishida, and M. Aoyagi, "Numerical study on acoustic oscillations of 2D and 3D flue organ pipe like instruments with compressible LES," *Acta Acustica united with Acustica* ***99***, 154-171 (2013).

[16] H. Yokoyama, A. Miki, H. Onitsuka, and A. Iida, "Direct numerical simulation of fluid-acoustic interactions in a recorder with tone holes," *J. Acoust. Soc. Amer.* **138**, 858-873 (2015); doi.org/10.1121/1.4926902.

[17] Y. Shi, A. R. da Silva, and G. P. Scavone, "LBM simulation of the quasi-static flow in a clarinet," Proceedings of the Third Vienna Talk on Music Acoustics, p. 35-42 (2015).

[18] S. Tateishi, S. Iwagami, G. Tsutsumi, T. Kobayashi, T. Takami, and K. Takahashi, "Role of foot chamber in the sounding mechanism of a flue organ pipe," *Acoust. Sci. & Tech.* **40**, 29-39 (2019); doi: 10.1250/ast.40.29.

[19] Experimentally, temporarily blocking the jet at the end of the channel was found to be the best way to directly produce a transition to C6; simply cycling the gasline pump off and on from the desired steady-state pressure/flow did not provide a fast enough ramp rate and consistently left the system in the C5 state.